Wave–Particle Duality in Swirl–String Theory: Toroidal Circulation, Knot Collapse, and Photon-Induced Transitions

Omar Iskandarani
Independent Researcher, Groningen, The Netherlands

January 17, 2026

Abstract

We present a Swirl–String Theory (SST) interpretation of the electron's wave–particle duality based on Canon v0.3.1. The electron is modeled as a swirl-string admitting two phases: an unknotted, delocalized toroidal circulation $\mathcal{R}$ (wave-like) and a localized, knotted soliton (trefoil) $\mathcal{T}$ (particle-like). We define an effective energy functional including bulk swirl density, line tension, near-contact interactions, and helicity terms. Photon-induced transitions $\mathcal{R} \rightleftarrows \mathcal{T}$ occur at resonant frequencies determined by impedance matching between electromagnetic modes and topological excitations. We show how circulation quantization on $\mathcal{R}$ recovers de Broglie wave relations, while $\mathcal{T}$ provides a stable, localized excitation. This framework yields falsifiable predictions in atomic absorption spectra, Rydberg scaling, and polarization-dependent selection rules.

1 Introduction

Wave–particle duality remains a central puzzle in quantum mechanics. The hydrodynamic representation of the Schrödinger equation by Madelung [4], the matter-wave hypothesis of de Broglie [7], and Bohm's hidden-variable interpretation [8, 9] all highlight fluid analogies. In superfluids, Onsager's circulation quantization [10] and Feynman's analysis of helium vortices [11] demonstrate how phase coherence enforces quantized flow. Earlier, Helmholtz [12] and Kelvin [13] established the conservation of vorticity and proposed atoms as vortex rings.

Within SST, the Canon postulates a universal swirl condensate with effective density ρ_f and characteristic swirl velocity $\|\mathbf{v}_\circlearrowleft\|$. Electrons are interpreted not as point particles but as filamentary swirl-strings. We propose here that the dual character of the electron arises from two distinct phases of the same underlying string.

2 Two Phases of the Electron String

2.1 Unknotted toroidal ring R

The delocalized phase is an unknotted ring circulation $\mathcal{R}$ with radius R and length $L(\mathcal{R}) = 2\pi R$. Its circulation is quantized:

$$\Gamma_n = \oint_{\mathcal{R}} \mathbf{v} \cdot d\boldsymbol{\ell} = n\frac{h}{m_e}, \qquad n \in \mathbb{Z}. \tag{1}$$

Hence the tangential speed is

$$v_\theta(R) = \frac{\Gamma_n}{2\pi R}, \tag{2}$$

and the phase around the ring is $e^{in\theta}$, yielding the de Broglie relation

$$\lambda_{ring} = \frac{2\pi R}{n} = \frac{h}{p_\theta}, \qquad p_\theta = m_e v_\theta. \tag{3}$$

Thus $\mathcal{R}$ naturally supports interference and standing-wave behavior.

2.2 Knotted trefoil soliton

The localized phase $\mathcal{T}$ is a knotted filament (e.g. trefoil 3_1) with enhanced curvature and helicity. Its invariants satisfy $C(\mathcal{T}) > 0$, $\mathcal{H}(\mathcal{T}) \neq 0$, and typically $L(\mathcal{T}) > L(\mathcal{R})$ for equal scale.

2.3 Effective energy functional

We postulate an effective energy functional

$$\boxed{\mathcal{E}_{eff}[K] = \underbrace{\epsilon_0 A L(K)}_{\text{bulk swirl energy}} + \underbrace{\beta L(K)}_{\text{line tension}} + \underbrace{\alpha C(K)}_{\text{near-contact}} + \underbrace{\gamma \mathcal{H}(K)}_{\text{helicity}}} \tag{4}$$

where K is the filament curve, $A = \pi r_c^2$ is the core cross-sectional area, and ϵ_0 is the Canon bulk energy density

$$\epsilon_0 = \frac{4}{\alpha_{\mathrm{fs}}\,\varphi} \left(\tfrac{1}{2}\rho_f \|\mathbf{v}_{\circlearrowleft}\|^2\right). \tag{5}$$

2.4 Dimensional analysis

- $[\epsilon_0] = \mathrm{J\,m^{-3}}$, $[A] = \mathrm{m^2}$, $[L] = \mathrm{m} \Rightarrow [\epsilon_0 A L] = \mathrm{J}$.
- $[\beta] = \mathrm{J\,m^{-1}}$, hence $[\beta L] = \mathrm{J}$.
- αC, $\gamma \mathcal{H}$ contribute as energy terms.

Numerically, with Canon constants,

$$\epsilon_0 \approx 1.4187 \times 10^8\ \mathrm{J\,m^{-3}}, \quad A \approx 6.24 \times 10^{-30}\ \mathrm{m^2}, \tag{6}$$

so bulk energy per length is

$$\epsilon_0 A \approx 8.85 \times 10^{-22}\ \mathrm{J\,m^{-1}}. \tag{7}$$

3 Photon-Driven Transitions

3.1 Resonance condition

The transition $\mathcal{R} \to \mathcal{T}$ changes the energy by

$$\Delta E = (\epsilon_0 A + \beta)\Delta L + \alpha C(\mathcal{T}) + \gamma \mathcal{H}(\mathcal{T}). \tag{8}$$

Resonance occurs when

$$\boxed{\hbar\omega \approx \Delta E}. \tag{9}$$

3.2 Selection rules

- Angular momentum matching: photon helicity must match the winding number (e.g. $\Delta n = \pm 3$ for trefoil).
- Radius dependence: larger R reduces ΔL, lowering resonance energy (Rydberg scaling).
- Polarization dependence: circular polarization aligned with knot chirality enhances coupling.

4 Effective Field Theory Formulation

At the EFT level, the string world-sheet Σ enters a Lagrangian

$$\mathcal{L} = \tfrac{1}{2}\rho_f \|\mathbf{v}\|^2 - \rho_E - \beta\ell[\Sigma] - \alpha\mathcal{C}[\Sigma] - \gamma\mathcal{H}[\Sigma] + \mathcal{L}_{\rm EM}^{int}[A_\mu;\Sigma]. \tag{10}$$

In the static limit, $\mathcal{L} \to -\mathcal{E}_{eff}$. Time-dependent solutions yield Rabi-like oscillations between $\mathcal{R}$ and $\mathcal{T}$ under monochromatic drive $\omega \approx \Delta E/\hbar$.

5 Photoelectric and Compton Effects from Canonical Photon Modes

5.1 Canonical Photon Mode Recap

From Sec. X (Canonical photon derivation), the photon is described as a *pulsed unknot swirl-string*, with action

$$S[\xi] = \tfrac{1}{2}\,\rho_f A_{\rm eff} \int dt \int_0^L ds\,\left[(\partial_t\xi)^2 - c^2(\partial_s\xi)^2\right],$$

normal modes $\xi_m(s,t)$ of frequency $\omega_m = ck_m$, and single-quantum amplitude

$$a_m = \sqrt{\frac{\hbar}{\rho_f\, A_{\rm eff}\, L\, \omega_m}}. \tag{11}$$

This constitutes the *canonical* photon description in SST: delocalized circulation with no rest-mass density ($\rho_m = 0$), but finite energy density ρ_E.

5.2 Swirl–EM Mapping (Empirical Consistency)

To compare with classical electrodynamics, we adopt the empirical swirl–EM map

$$\mathbf{E} = \sqrt{\frac{\rho_f}{\varepsilon_0}}\,\mathbf{v}, \qquad \mathbf{B} = \sqrt{\frac{\rho_f}{\varepsilon_0}}\,\mathbf{b}, \qquad \omega = ck, \tag{12}$$

so that the quadratic energy–momentum balance reproduces Maxwell:

$$u = \tfrac{\varepsilon_0}{2}E^2 + \tfrac{1}{2\mu_0}B^2, \qquad \mathbf{S} = \mu_0^{-1}\mathbf{E}\times\mathbf{B},$$

with $c^{-2} = \varepsilon_0\mu_0$ [18]. Equation (11) is then consistent with the cavity-QED single-photon field amplitudes [19, 20].

5.3 Photoelectric Effect as $\mathcal{R}\to\mathcal{T}$ Transition

Within the $\mathcal{R}/\mathcal{T}$ two-phase electron model (SST-1), absorption of a canonical photon mode by a delocalized electron $\mathcal{R}$ can trigger localization to a knotted $\mathcal{T}$ state if

$$\hbar\omega \;\geq\; \Phi + \Delta E_{RT}, \tag{13}$$

where Φ is the material work function and $\Delta E_{RT} = E[\mathcal{T}] - E[\mathcal{R}]$ the localization gap. In metals, ΔE_{RT} is negligible or renormalized into an effective Φ_{eff}, giving Einstein's law

$$K_{\rm max} = \hbar\omega - \Phi_{eff}. \tag{14}$$

This is thus recovered as an *empirical consequence* of the canonical photon.

5.4 Compton Scattering with a Delocalized Photon Packet

Treating the incident photon as a canonical delocalized mode of momentum $(\hbar\omega/c,\ \hbar\mathbf{k})$ and the target electron as a localized $\mathcal{T}$ of mass m_e, energy–momentum conservation gives

$$\Delta\lambda = \lambda' - \lambda = \frac{h}{m_e c}\,(1 - \cos\theta), \tag{15}$$

the standard Compton shift [16]. The equality follows because the swirl–EM map (12) preserves stress–energy flux.

5.5 Consistency, Limits, and Corrections

Finite core structure of the electron string introduces corrections $\mathcal{O}((kr_c)^2)$, negligible for $kr_c \ll 1$ (X-rays) but potentially testable at γ-ray energies.

Interpretation.

1. **Photoelectric:** canonical photon $\rightarrow$ delocalized $\mathcal{R}$ electron $\rightarrow$ localized $\mathcal{T}$ emission.
2. **Compton:** canonical photon scattering on $\mathcal{T}$ electron, kinematics as in QED.
3. **Polarization:** photon helicity corresponds to swirl-clock orientation, affecting cross sections and selection rules.

5.6 Notes on Provenance

- Einstein's photoelectric law [14, 15].
- Compton scattering and Klein–Nishina [16, 17].
- Swirl–EM map consistency with Maxwell [18].
- Cavity QED amplitudes [19, 20].

6 Predictions and Tests

1. **Spectral lines:** new resonances in absorption spectra, not coinciding with standard atomic transitions.
2. **Rydberg atoms:** red-shifted knotting lines with increasing principal quantum number.
3. **Pump–probe:** suppression of interference fringes coincident with localization after resonant pump.
4. **Polarization dependence:** transition rates sensitive to photon chirality.

7 Conclusion

In SST, the same electron string supports both a delocalized circulation $\mathcal{R}$ (wave aspect) and a localized knot $\mathcal{T}$ (particle aspect). Photon-induced transitions between these phases provide a dynamical explanation of wave–particle duality consistent with the Canon and with hydrodynamic analogies established since Helmholtz and Kelvin. The framework yields concrete, falsifiable predictions.

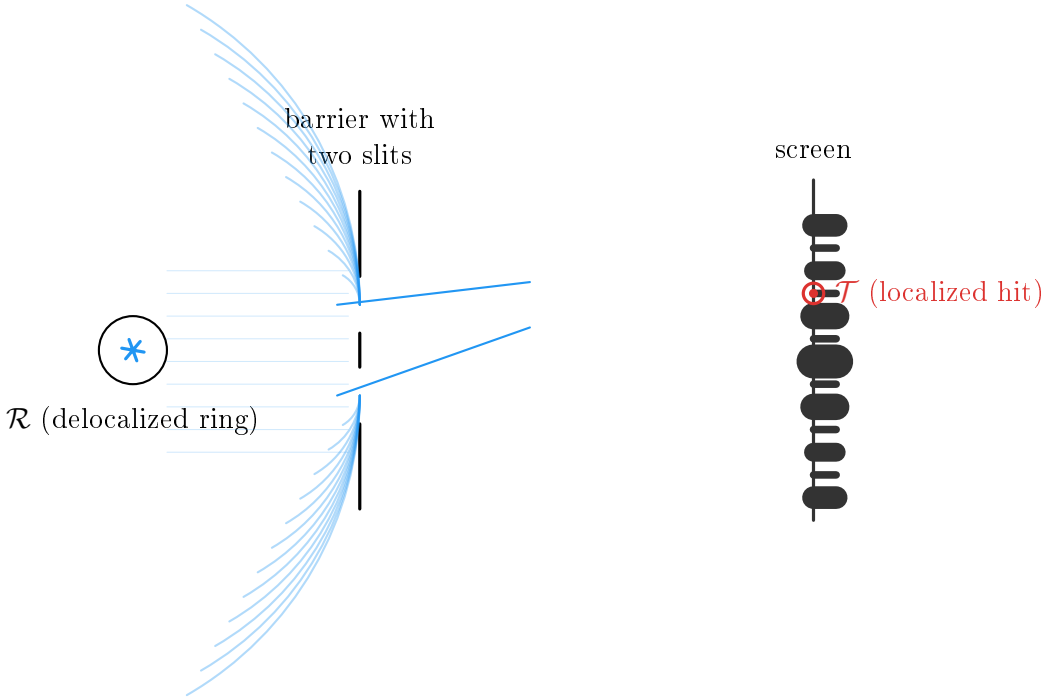

Figure 1: SST double slit schematic. The electron approaches as a delocalized toroidal circulation $\mathcal{R}$ (ring), whose phase bifurcates at two slits to produce coherent downstream fields that interfere. At the screen, interaction triggers collapse into a localized knotted state $\mathcal{T}$, yielding discrete impacts while the ensemble reproduces the fringe intensity.

Appendix: Popular Summary

A swirl-ring can ripple smoothly like a hula-hoop (wave). If twisted into a knot, the swirl bunches up in one spot (particle). A photon of just the right frequency can flip the string between these two states.

A Quantitative Fringe Geometry and Visibility

Consider a double slit with center-to-center separation s and distance L from slits to screen. Let the electron approach in the delocalized ring phase $\mathcal{R}$ with mean axial momentum p_z (de Broglie wavelength $\lambda = h/p_z$). In the Fraunhofer regime ($L \gg s^2/\lambda$), the transverse intensity on the screen is well approximated by

$$I(x) \;\propto\; I_1(x) + I_2(x) + 2\sqrt{I_1(x) I_2(x)}\,\cos\!\Big(\tfrac{2\pi s}{\lambda}\tfrac{x}{L} + \phi_0\Big), \tag{16}$$

with fringe spacing

$$\boxed{\,d \;=\; \frac{\lambda L}{s}\,}. \tag{17}$$

Within SST, the phase ϕ_0 is the circulation phase offset inherited from $\mathcal{R}$; any path-dependent coupling to the environment adds a random phase $\delta\phi$ that reduces the fringe visibility

$$\mathcal{V} \equiv \frac{I_{\max} - I_{\min}}{I_{\max} + I_{\min}} \;=\; \big|\langle e^{i\delta\phi}\rangle\big|. \tag{18}$$

A.1 Ring-phase mapping

For the ring state $\mathcal{R}$ with quantized azimuthal phase $e^{in\theta}$, the two slits act as partial projectors of this phase onto two spatially separated downstream wavefronts. The resulting interference encodes the *same* azimuthal winding through the optical path difference $\Delta\ell(x) \approx s\,x/L$, hence the cosine argument above.

B Which-Way Coupling and Decoherence in SST

In SST language, "which-way" monitoring is an *EM impedance* to the ring phase, parameterized by a coupling rate Γ (net photon or field-interaction rate that carries path information). Let τ be the transit time through the interferometer. For weak, memoryless monitoring the phase undergoes a random walk, giving the standard exponential visibility law [21]

$$\boxed{\mathcal{V}(\Gamma,\tau) \;=\; e^{-\Gamma\tau}}. \tag{19}$$

Equivalently, define a *monitoring strength* $\eta \in [0,1]$ as the single-pass which-way information; then $\mathcal{V} = \sqrt{1-\eta}$ (two-outcome, information-balance form). Both parameterizations are compatible at small η via $\eta \simeq 2(1-e^{-\Gamma\tau})$.

SST mechanism. Microscopically, the EM coupling stochastically seeds premature $\mathcal{R}\to\mathcal{T}$ collapses *upstream*, terminating coherent superposition. Equation (19) thus measures the survival probability of coherence before the knotting transition.

B.1 Dimensional check

Γ has units s^{-1} and τ has units s, so $\Gamma\tau$ is dimensionless, consistent with (19).

C Delayed-Choice and Quantum Eraser (SST View)

In a Wheeler-type delayed choice, the interferometer is reconfigured *after* the electron passes the slits [22]. In SST, this reconfiguration alters whether the downstream optics *allow* continued $\mathcal{R}$-phase recombination or instead force local $\mathcal{T}$-phase collapse:

- **Interference mode on:** downstream optics preserve the $\mathcal{R}$ phase coherence until the screen $\Rightarrow$ fringes.
- **Which-way mode on:** downstream optics couple EM impedance strongly, enforcing premature $\mathcal{R}\to\mathcal{T}$ collapse $\Rightarrow$ no fringes.

A quantum eraser removes the stored which-way information, effectively *post-selecting* runs where $\mathcal{R}$-coherence survived to the recombination stage; sorted sub-ensembles then display fringes.

D Spectroscopic Rabi Drive Between $\mathcal{R}$ and $\mathcal{T}$

We model the $\mathcal{R}\leftrightarrow\mathcal{T}$ manifold as a driven two-level system with detuning $\Delta = \omega - \omega_0$ (where $\hbar\omega_0 = \Delta E_{\mathcal{R}\to\mathcal{T}}$) and coupling Ω_R set by the EM impedance overlap:

$$\dot{c}_{\mathcal{R}} = -\tfrac{i}{2}\Omega_R c_{\mathcal{T}} - \tfrac{\gamma_{\mathcal{R}}}{2} c_{\mathcal{R}}, \tag{20}$$

$$\dot{c}_{\mathcal{T}} = -\tfrac{i}{2}\Omega_R c_{\mathcal{R}} - \Big(\tfrac{\gamma_{\mathcal{T}}}{2} + i\Delta\Big) c_{\mathcal{T}}. \tag{21}$$

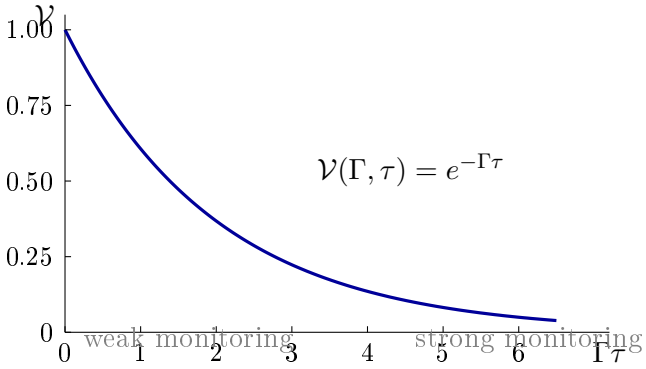

Figure 2: Fringe visibility vs. which-way coupling in SST. The parameter Γ encodes EM impedance to the $\mathcal{R}$ phase (path information rate), τ is the transit time. Exponential decay of visibility reflects coherence loss prior to recombination.

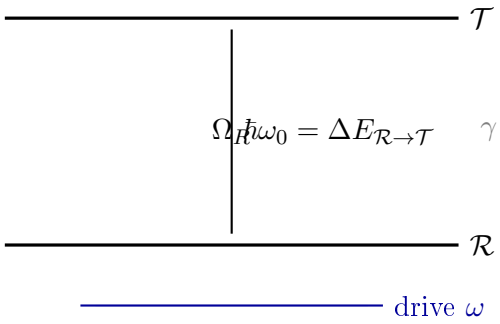

Figure 3: Two-level SST manifold for $\mathcal{R} \leftrightarrow \mathcal{T}$ with Rabi drive. At resonance $\omega = \omega_0$, the knotting probability oscillates at Ω_R and decays at rate γ, enabling pump–probe control of collapse within an interferometer.

At resonance ($\Delta = 0$) and for $\gamma_{\mathcal{R}}, \gamma_{\mathcal{T}} \ll \Omega_R$,

$$P_{\mathcal{T}}(t) = |c_{\mathcal{T}}(t)|^2 \;=\; \sin^2\!\Big(\frac{\Omega_R t}{2}\Big)\, e^{-\gamma t}, \qquad \gamma \equiv \tfrac{\gamma_{\mathcal{R}}+\gamma_{\mathcal{T}}}{2}. \tag{22}$$

A *pump–probe* synchronized to the flight time across the interferometer can therefore *gate* the knotting probability and modulate fringe visibility in a time-resolved fashion.

Boxed Result (SST double slit). An electron is a single swirl-string with two phases: $\mathcal{R}$ (delocalized ring) for propagation and $\mathcal{T}$ (knotted soliton) for detection. Interference arises from coherent splitting and recombination of $\mathcal{R}$; localized impacts result from $\mathcal{R} \to \mathcal{T}$ collapse at the screen. Which-way monitoring increases the EM impedance, raising the premature knotting rate Γ; the fringe visibility obeys $\mathcal{V} = e^{-\Gamma\tau}$ and vanishes in the strong-monitoring limit.

References

[1] William Thomson (Lord Kelvin). On Vortex Atoms. Proceedings of the Royal Society of Edinburgh, 6:94–105, 1867. `https://zapatopi.net/kelvin/papers/on_vortex_atoms.html`

[2] G. K. Batchelor. An Introduction to Fluid Dynamics. Cambridge University Press, 1967. doi:10.1017/CBO9780511800955

[3] P. G. Saffman. Vortex Dynamics. Cambridge University Press, 1992. doi:10.1017/CBO9780511624063

[4] E. Madelung. Quantentheorie in hydrodynamischer Form. Zeitschrift für Physik, 40:322–326, 1927. doi:10.1007/BF01400372

[5] A. L. Fetter. Quantum Theory of Superfluid Vortices. I. Liquid Helium II. Physical Review, 162:143–153, 1967. doi:10.1103/PhysRev.162.143

[6] Andrés Corrada-Emmanuel. Algebraic topology and the quantization of circulation in superfluid helium. Physical Review B, 45:2553–2556, 1992. doi:10.1103/PhysRevB.45.2553

[7] L. de Broglie. Recherches sur la théorie des quanta. Annales de Physique, 3(10):22–128, 1925. doi:10.1051/anphys/192510030022.

[8] D. Bohm. A Suggested Interpretation of the Quantum Theory in Terms of "Hidden" Variables I. Phys. Rev., 85(2):166–179, 1952. doi:10.1103/PhysRev.85.166.

[9] D. Bohm. A Suggested Interpretation of the Quantum Theory in Terms of "Hidden" Variables II. Phys. Rev., 85(2):180–193, 1952. doi:10.1103/PhysRev.85.180.

[10] L. Onsager. Statistical hydrodynamics. Il Nuovo Cimento (Supplemento), 6:279–287, 1949. doi:10.1007/BF02780991.

[11] R. P. Feynman. Application of Quantum Mechanics to Liquid Helium. In C. J. Gorter, editor, Progress in Low Temperature Physics, Vol. I, pages 17–53. North-Holland, 1955. doi:10.1016/S0079-6417(08)60077-3.

[12] H. von Helmholtz. Über Integrale der hydrodynamischen Gleichungen, welche den Wirbelbewegungen entsprechen. Journal für die reine und angewandte Mathematik, 55:25–55, 1858. doi:10.1515/crll.1858.55.25.

[13] W. Thomson (Lord Kelvin). On Vortex Motion. Transactions of the Royal Society of Edinburgh, 25:217–260, 1869.

[14] A. Einstein. On a Heuristic Viewpoint Concerning the Production and Transformation of Light. Annalen der Physik, 1905.

[15] R. A. Millikan. A Direct Photoelectric Determination of Planck's h. Physical Review, 7:355–388, 1916. doi:10.1103/PhysRev.7.355.

[16] A. H. Compton. A Quantum Theory of the Scattering of X-Rays by Light Elements. Physical Review, 21:483–502, 1923. doi:10.1103/PhysRev.21.483.

[17] O. Klein and Y. Nishina. Über die Streuung von Strahlung durch freie Elektronen nach der neuen relativistischen Quantendynamik von Dirac. Zeitschrift für Physik, 52:853–868, 1929. doi:10.1007/BF01366453.

[18] J. D. Jackson. Classical Electrodynamics, 3rd Edition. Wiley, 1999. ISBN: 9780471309321.

[19] S. Haroche and J.-M. Raimond. Exploring the Quantum: Atoms, Cavities, and Photons. Oxford University Press, 2006. ISBN: 9780198509141.

[20] M. O. Scully and M. S. Zubairy. Quantum Optics. Cambridge University Press, 1997. ISBN: 9780521435956.

[21] W. H. Zurek, Decoherence, einselection, and the quantum origins of the classical, *Rev. Mod. Phys.* **75**(3), 715–775 (2003). doi:10.1103/RevModPhys.75.715

[22] J. A. Wheeler, The 'Past' and the 'Delayed-Choice' Double-Slit Experiment, in *Mathematical Foundations of Quantum Theory*, ed. A. R. Marlow, Academic Press, New York, 1978, pp. 9–48.